




# Assessment of Clofazimine and TB47 Combination Activity against *Mycobacterium abscessus* Using a Bioluminescent Approach

Yang Liu,<sup>a</sup> Yaoju Tan,<sup>b</sup> M. Mahmudul Islam,<sup>a,c</sup> Yuanyuan Cao,<sup>a</sup> Xiaoyun Lu,<sup>d</sup> Sheng Zeng,<sup>a</sup> H. M. Adnan Hameed,<sup>a,c</sup> Peipei Zhou,<sup>a</sup> Xingshan Cai,<sup>b</sup> Shuai Wang,<sup>a,c</sup> Julius N. Mugweru,<sup>a,c,e</sup> Guoliang Zhang,<sup>f</sup> Huancai Yin,<sup>g</sup> Jianxiong Liu,<sup>b</sup> Eric Nuermberger,<sup>h</sup>  Tianyu Zhang<sup>a,c</sup>

<sup>a</sup>State Key Laboratory of Respiratory Disease, Guangzhou Institutes of Biomedicine and Health, Chinese Academy of Sciences, Guangzhou, China

<sup>b</sup>State Key Laboratory of Respiratory Disease, Department of Clinical Laboratory, Guangzhou Chest Hospital, Guangzhou, China

<sup>c</sup>University of Chinese Academy of Sciences, Beijing, China

<sup>d</sup>School of Pharmacy, Jinan University, Guangzhou, China

<sup>e</sup>Department of Biological Sciences, University of Embu, Embu, Kenya

<sup>f</sup>Guangdong Key Laboratory of Emerging Infectious Diseases, Shenzhen Third People's Hospital, Southern University of Science and Technology, Shenzhen, China

<sup>g</sup>Chinese Academy of Sciences Key Laboratory of Bio-Medical Diagnostics, Suzhou Institute of Biomedical Engineering and Technology, Chinese Academy of Sciences, Jiangsu, China

<sup>h</sup>Center for Tuberculosis Research, Department of Medicine, Johns Hopkins University, Baltimore, Maryland, USA

Yang Liu, Yaoju Tan, M. Mahmudul Islam, Yuanyuan Cao, and Xiaoyun Lu contributed equally to this work. Author order was determined in order of increasing seniority.

**ABSTRACT** *Mycobacterium abscessus* is intrinsically resistant to most antimicrobial agents. The emerging infections caused by *M. abscessus* and the lack of effective treatment call for rapid attention. Here, we intended to construct a selectable marker-free autoluminescent *M. abscessus* strain (designated UAIMab) as a real-time reporter strain to facilitate the discovery of effective drugs and regimens for treating *M. abscessus*. The UAIMab strain was constructed using the *dif*/Xer recombinase system. *In vitro* and *in vivo* activities of several drugs, including clofazimine and TB47, a recently reported cytochrome *bc<sub>1</sub>* inhibitor, were assessed using UAIMab. Furthermore, the efficacy of multiple drug combinations, including the clofazimine and TB47 combination, were tested against 20 clinical *M. abscessus* isolates. The UAIMab strain enabled us to evaluate drug efficacy both *in vitro* and in live BALB/c mice in a real-time, noninvasive fashion. Importantly, although TB47 showed marginal activity either alone or in combination with clarithromycin, amikacin, or roxithromycin, the drug markedly potentiated the activity of clofazimine, both *in vitro* and *in vivo*. This study demonstrates that the use of the UAIMab strain can significantly facilitate rapid evaluation of new drugs and regimens. The clofazimine and TB47 combination is effective against *M. abscessus*, and dual/triple electron transport chain (ETC) targeting can be an effective therapeutic approach for treating mycobacterial infections.

**KEYWORDS** *Mycobacterium abscessus*, cytochrome *bc<sub>1</sub>* inhibitor, TB47, clofazimine, autoluminescent

*Mycobacterium abscessus*, a rapidly growing nontuberculous mycobacterium (NTM), is an important epidemiological agent causing opportunistic infections in human lungs, skin, and soft tissues, leading to significant morbidity and even mortality (1, 2). Notably, structural lung diseases such as cystic fibrosis and chronic obstructive pulmonary disease are important risk factors potentiating *M. abscessus* infection. Indeed, it has

**Citation** Liu Y, Tan Y, Islam MM, Cao Y, Lu X, Zeng S, Hameed HMA, Zhou P, Cai X, Wang S, Mugweru JN, Zhang G, Yin H, Liu J, Nuermberger E, Zhang T. 2020. Assessment of clofazimine and TB47 combination activity against *Mycobacterium abscessus* using a bioluminescent approach. *Antimicrob Agents Chemother* 64:e01881-19. <https://doi.org/10.1128/AAC.01881-19>.

**Copyright** © 2020 American Society for Microbiology. All Rights Reserved.

Address correspondence to Tianyu Zhang, zhang\_tianyu@gibh.ac.cn.

**Received** 16 September 2019

**Returned for modification** 11 October 2019

**Accepted** 10 December 2019

**Accepted manuscript posted online** 16 December 2019

**Published** 21 February 2020

been reported that between 16% to 68% cases of cystic fibrosis are further complicated by *M. abscessus* infection (3).

*M. abscessus* infection is difficult to treat due to its intrinsic resistance to most of the available antibiotics, including the classic antitubercular drugs (4). Current medical intervention of *M. abscessus* infection depends on combinational chemotherapy with drugs belonging to different groups, e.g., amikacin, clarithromycin or azithromycin, imipenem, and cefoxitin (4). Unfortunately, treatment failure occurs frequently despite prolonged administration of these antibiotics. Furthermore, current treatment regimens are often associated with severe side effects (4). Therefore, development of new drugs and regimens is urgently needed to facilitate the eradication of *M. abscessus* infection.

A series of drug candidates are currently under evaluation for tuberculosis treatment (5). This is exemplified by clofazimine, a riminophenazine drug that was originally prescribed for leprosy and now repurposed for tuberculosis treatment. Clofazimine was reported to compete with menaquinone by shuttling electrons from type II NADH dehydrogenase (NDH-2) to oxygen, leading to the generation of lethal levels of reactive oxygen species (ROS) (6). Possibly due to this unique mode of action, the drug is effective against multidrug-resistant *Mycobacterium tuberculosis* strains (7, 8). In addition to *M. tuberculosis*, clofazimine was also found to exert potent activity either alone or in combination with amikacin or clarithromycin against *M. abscessus* *in vitro* (9). Furthermore, a recent retrospective study also supported the use of clofazimine-containing regimens in the treatment of human *M. abscessus* infection (10). Thus, clofazimine seems to be a valuable drug for coping with *M. abscessus* infection. However, it should be noted that clofazimine has a delayed activity against *M. tuberculosis* both *in vitro* and *in vivo* (11). It is yet unknown whether the antimicrobial activity of clofazimine is also delayed against *M. abscessus*. Furthermore, long-term *in vivo* activity of clofazimine against this bacterium, to our knowledge, has not been reported.

In addition to clofazimine, the current antituberculosis drug discovery pipeline (5) also includes other mycobacterial electron transport chain (ETC)-targeting drugs, such as Q203 inhibiting QcrB in the cytochrome *bc*<sub>1</sub> complex (12). We reported a series of pyrazolo[1,5-*a*]pyridine-3-carboxamide derivatives as active compounds against both drug-susceptible and multidrug-resistant *M. tuberculosis* strains (13). The lead compound of this series, i.e., TB47, showed excellent therapeutic activity in a mouse model of *Mycobacterium ulcerans* infection (14) and is now considered a promising antituberculosis drug candidate (<http://www.newtdrugs.org/pipeline/discovery>). Similar to Q203, TB47 also targets the QcrB protein, thereby inhibiting the activity of the cytochrome *bc*<sub>1</sub>-*aa*<sub>3</sub> supercomplex (14, 15).

Interestingly, combination treatment of clofazimine with cytochrome *bc*<sub>1</sub> inhibitors (e.g., Q203) was demonstrated to deliver a markedly enhanced killing of both replicating and nonreplicating *M. tuberculosis* bacteria (16, 17). Furthermore, inhibitors of menaquinone biosynthesis also have enhanced activity when administered in combination with other ETC-targeting drugs, such as clofazimine and QcrB inhibitors (18). These findings emphasize dual-ETC targeting as a novel antitubercular strategy. This strategy has not been evaluated against *M. abscessus*. In this study, we, for the first time, constructed a selectable marker-free autoluminescent *M. abscessus* strain. Autoluminescent strains of *M. tuberculosis*, *M. ulcerans*, and *M. abscessus* have been constructed previously (19–21), allowing for more facile, real-time, and noninvasive assessment of antibiotic activity both *in vitro* and *in vivo*. Notably, the previously described autoluminescent *M. abscessus* strain harbors a selection marker (21). Using the selectable marker-free autoluminescent *M. abscessus* strain (designated strain UAIMab) constructed in this study, we further evaluated the efficacy of various drugs and combinations, with a focus on the clofazimine and TB47 combination, against *M. abscessus* both *in vitro* and *in vivo*.

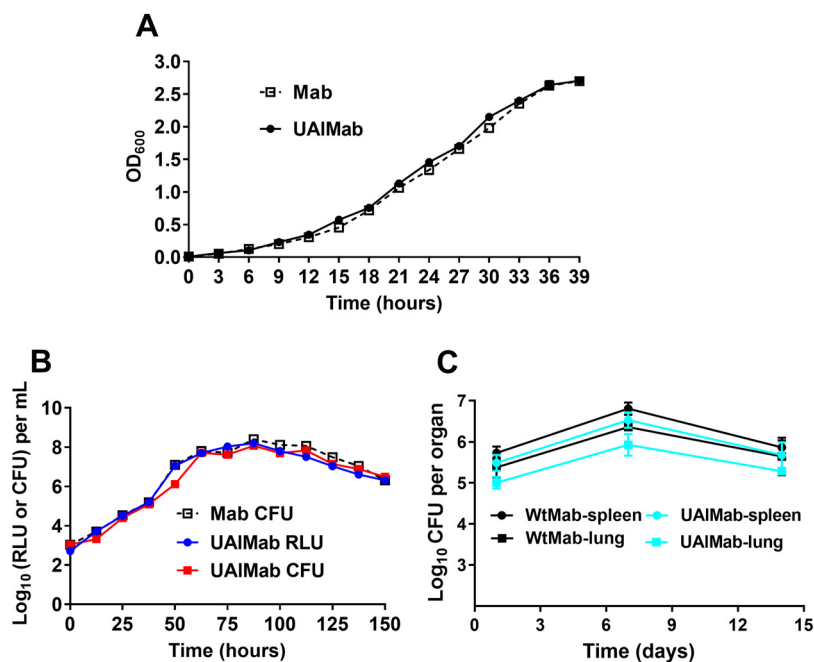


**FIG 1** The growth of the UAImab strain is comparable to that of the parental *M. abscessus* (Mab) strain. Growth curves of bacteria in 7H9 medium with 0.05% Tween 80 were monitored by the OD<sub>600</sub> (A) and CFU and RLU measurement (B) at indicated time points. (C) Nude mice were infected via tail vein with UAImab or the parental strain, WT *M. abscessus* (WtMab), followed by assessment of bacterial burden in lungs and spleens by CFU counting. These experiments were performed three times. Data from one representative experiment are shown.

## RESULTS

**Engineering of UAImab suitable for antibiotic screening.** Using the *Xer/dif* system, we first constructed a selectable marker-free, autoluminescent *M. abscessus* strain expressing the *luxCDABE* operon for facile and real-time evaluation of antibiotic efficacy, as described earlier in *M. tuberculosis* (19, 22). The construction and further stability assessment of the UAImab strain are detailed in the supplemental material.

We compared the growth of UAImab with that of its parental strain. It was observed that under *in vitro* conditions, the growth of UAImab, judged by the optical density at 600 nm (OD<sub>600</sub>) (Fig. 1A) and CFU counts (Fig. 1B), was similar to that of the parental strain. Furthermore, the growth pattern of UAImab was also comparable to that of the parental strain in immunocompromised nude mice (Fig. 1C). We also monitored the growth kinetics of the UAImab culture by measuring the relative light units (RLU). The result showed that the RLU curve of UAImab fitted well with its CFU curve (Fig. 1B). Therefore, RLU counts can be used as an indicator of bacterial growth for UAImab.

The comparable growth of UAImab rendered this reporter strain suitable for antibiotic evaluation. However, prior to its application, it was necessary to determine if general antibiotic susceptibility was altered in this reporter strain. We therefore compared the MICs of various drugs with distinct modes of action (i.e., clarithromycin, amikacin, clofazimine, and cefoxitin) against both UAImab and the parental strain using the conventional agar proportion method. As shown in Table 1, the MICs of these drugs determined for UAImab were identical to those determined for the parental strain, suggesting that the general antibiotic susceptibility is not altered in the UAImab strain. Given that the use of autoluminescent *M. tuberculosis* and *M. ulcerans* in antibiotic susceptibility testing can offer considerable advantages, such as real-time detection and cost efficiency (19, 20), we interrogated if RLU measurement using the UAImab strain could be applied as a surrogate methodology for antibiotic evaluation in *M. abscessus*. Thus, RLU counts in UAImab culture in the presence of various concentrations of clarithromycin, amikacin, clofazimine, or cefoxitin were monitored. Represen-

**TABLE 1** MICs determined by the agar proportion method<sup>a</sup>

Antibiotic	MIC (mg/liter)	
	WT <i>M. abscessus</i>	UAIMab
Clofazimine	2	2
Amikacin	4	4
Clarithromycin	4	4
Cefoxitin	32	32

<sup>a</sup>Results were recorded at 4 days postinoculation.

tative data shown in Fig. 2 demonstrated that MICs obtained by measuring RLU were comparable to those by conventional assay (Table 1), suggesting that RLU measurement of UAIMab is both valid and reliable for antibiotic susceptibility testing. However, considering that the MICs could be obtained as early as 6 h postinoculation in a small volume (e.g.,  $\leq 200 \mu\text{l}$ ) for the luminescence-based assay (Fig. 2), in sharp contrast to the 4 days required for conventional agar-based method, we propose that the UAIMab strain be used as a surrogate reporter strain in future screening and evaluation of new anti-*M. abscessus* drug candidates.

**TB47 and clofazimine combination is effective against *M. abscessus* in vitro.** The treatment of *M. abscessus* infections is now challenged by limited options of effective drugs and by the emergence of drug-resistant strains (4, 23). Clofazimine, clarithromycin, and amikacin were active against UAIMab (Table 1 and Fig. 2). We were interested to know whether their activity could be further potentiated by the QcrB-targeting TB47, discovered and reported recently by us (14, 15). In particular, given that combinations of mycobacterial ETC-targeting drugs were shown to yield markedly enhanced efficacy against *M. tuberculosis* (16–18), we wondered whether the TB47 and clofazimine

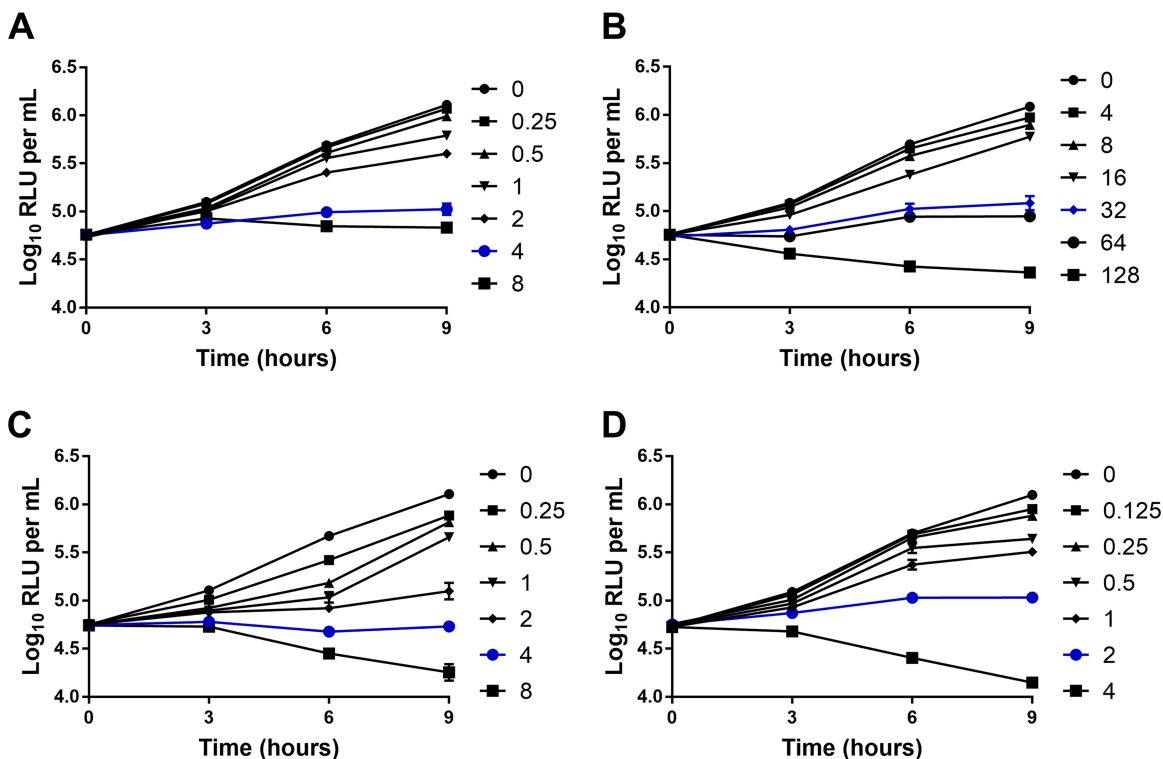


**FIG 2** Luminescence-based antibiotic susceptibility testing using UAIMab. Precultures of UAIMab were diluted to  $10^6$  CFU/ml in 7H9 medium containing 0.2% glycerol prior to the addition of various concentrations (mg/liter) of amikacin (A), cefoxitin (B), clarithromycin (C), and clofazimine (D). The luminescence was recorded at 0, 3, 6, and 9 h post-drug treatment. Representative data from one experiment performed in triplicate are shown. Error bars represent the standard deviations. The curves indicating the MICs of these drugs are shown in blue.

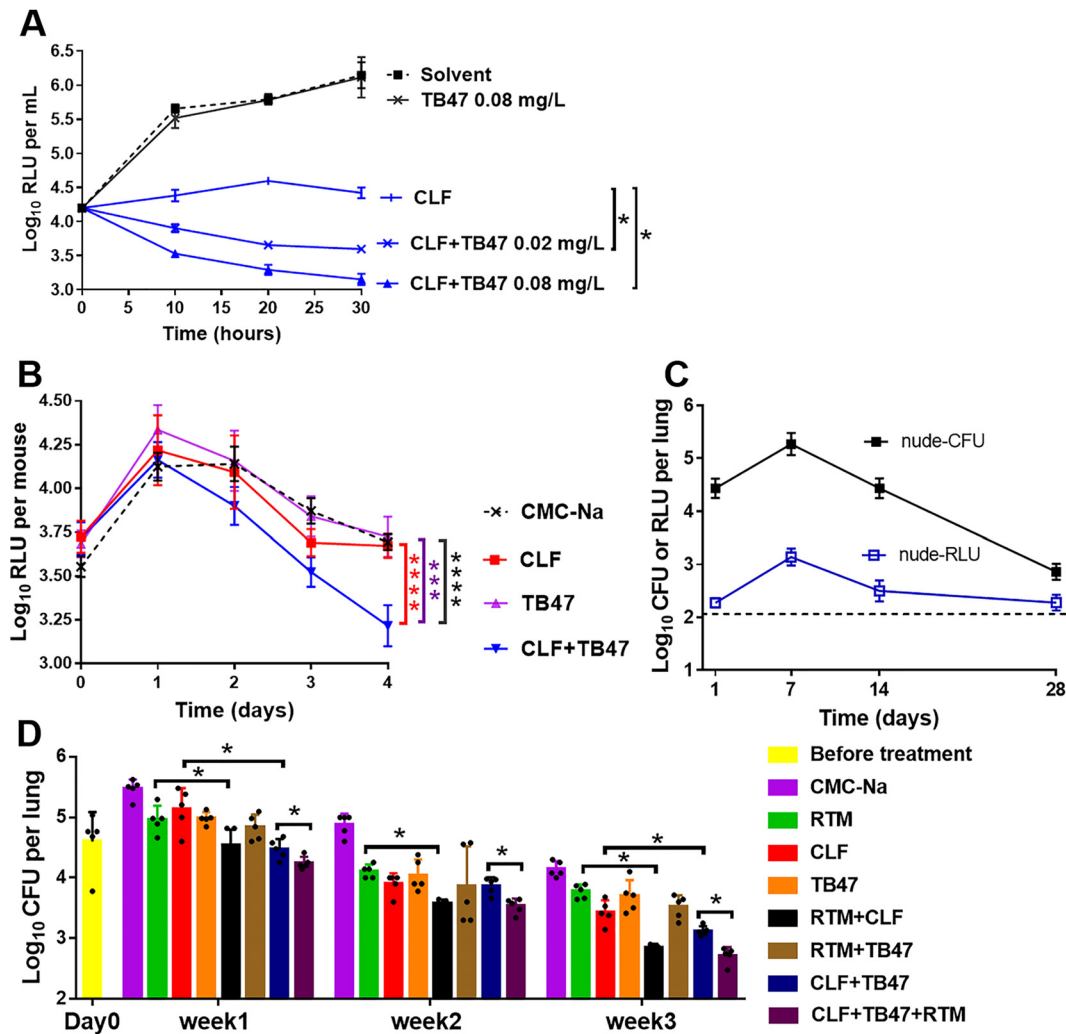


**FIG 3** Clofazimine-TB47 combination is effective against *M. abscessus*. (A) UAIMab was treated with TB47 (0.02 and 0.08 mg/liter), clofazimine (CLF; 2 mg/liter), or the drug combinations *in vitro*, and RLU counts were recorded at the indicated time points. \*,  $P < 0.05$  (unpaired *t* test). (B) Nude mice were infected via tail vein with UAIMab and treated with 0.05% CMC-Na (negative control), clofazimine (20 mg/kg/day), and/or TB47 (25 mg/kg/day). RLU counts were recorded from the breast of live mice consecutively for 4 days. \*\*\*,  $P < 0.001$ ; \*\*\*\*,  $P < 0.0001$  (unpaired *t* test). (C) Nude mice were aerosol infected with UAIMab, and bacterial burdens in lungs were monitored for 4 weeks by CFU and RLU measurements. (D) Nude mice were subject to aerosol infection of UAIMab and then treated with 0.05% CMC-Na, clofazimine (50 mg/kg/day), roxithromycin (RTM; 120 mg/kg/day), and TB47 (25 mg/kg/day). Bacterial burdens in lungs were assessed by CFU counting. \*,  $P < 0.05$  (unpaired *t* test).

combination could be effective against *M. abscessus*. We noted that TB47 had no obvious effect on the RLU values of UAIMab *in vitro* even at 50 mg/liter (Fig. 3A and data not shown), suggesting that TB47 alone had no discernible activity under this condition. Unlike TB47, clofazimine alone inhibited the increase in the RLU counts during growth (Fig. 3A), suggesting that this drug is effective against *M. abscessus* under this condition. Importantly, the combination of clofazimine with only 0.02 or 0.08 mg/liter TB47 gradually decreased the RLU counts (Fig. 3A), implying that this drug combination may kill *M. abscessus* efficiently. In contrast to activity of clofazimine, the activity of amikacin and two macrolides (clarithromycin and roxithromycin) was not potentiated by TB47 (data not shown).

#### Assessment of drug efficacy in a murine model of acute *M. abscessus* infection.

The growth of the UAIMab strain in mice was similar to that of the parental strain (Fig. 1C), allowing us to evaluate the efficacy of drug combinations in a mouse model through a noninvasive approach, as described earlier in *M. tuberculosis* (19). Acute



*M. abscessus* infection was initiated by infecting nude mice via tail vein with  $7.5 \log_{10}$  CFU of the parental strain or the UAIMab strain. We found that RLU counts in lungs of mice infected with UAIMab were 1.5 to  $2 \log_{10}$  greater than background values (i.e., data obtained with mice infected or not with the parental strain [data not shown]). Therefore, we could apply this noninvasive approach to evaluate drug efficacy in mice.

We observed that although treatment with clofazimine or TB47 had a marginal effect on the RLU curve relative to that of the control group, the combination of the two drugs markedly decreased the RLU value, particularly at 4 days postinfection (Fig. 3B). Therefore, the clofazimine and TB47 combination appears to be effective against *M. abscessus in vivo*.

**Assessment of drug efficacy in a murine model of *M. abscessus* pulmonary infection.** To further corroborate that the combination of clofazimine and TB47 is effective against *M. abscessus*, we applied a murine model of *M. abscessus* pulmonary infection using immunocompromised nude mice. Both CFU and RLU counting revealed an initial increase of bacterial burden in the lungs of the infected mice within the first week of infection and, thereafter, a decrease (Fig. 3C). In this model, treatment with roxithromycin slightly decreased bacterial burden in mouse lung (Fig. 3D). Clofazimine was found to decrease the CFU count only after 2 and 3 weeks of treatment (Fig. 3D), suggesting that clofazimine has a delayed effect against *M. abscessus*. In addition, bacterial burden in mice treated with TB47 was lower than that of the untreated controls (Fig. 3D), suggesting that TB47 alone has activity against *M. abscessus in vivo*.

We further tested various drug combinations (Fig. 3D) and observed that the combination of roxithromycin and clofazimine was more potent in decreasing bacterial burden than either drug alone. In contrast, the combination of roxithromycin and TB47 did not show any enhanced activity. Consistent with the data obtained from our *in vitro* study and the acute infection model (Fig. 3A and B), the combination of clofazimine and TB47 demonstrated augmented activity relative to that of either drug alone (Fig. 3D), emphasizing the efficacy of this combination in the treatment of *M. abscessus* infection. Since the combination of clofazimine with TB47 or roxithromycin had better activity (Fig. 3D), we further tested the efficacy of a clofazimine-TB47-roxithromycin triple combination. Relative to the activity of the clofazimine-TB47 combination, the triple combination delivered a slightly but significantly enhanced activity. Treatment with the triple combination was found to decrease bacterial burden in lung by  $>1 \log_{10}$  CFU compared to that of the control (Fig. 3D).

In the applied pulmonary infection model, bacterial burden in untreated mice began to decrease after 1 week of infection (Fig. 3C and D). This auto-clearing of bacterial loads may complicate the interpretation of our results. To further demonstrate the efficacy of treatment, we calculated and compared the rates of decrease in lung bacterial burden. As shown in Fig. S1 in the supplemental material, treatment with TB47 slightly boosted bacterial clearance relative to the level in the control. Treatment with clofazimine, the clofazimine-roxithromycin combination, the TB47-clofazimine combination, and the triple combination led to bacterial clearance 1.7-, 1.7-, 1.4-, and 1.5-fold faster than that of the solvent control. Thus, these drug combinations are effective against *M. abscessus*.

**Assessment of efficacy against 20 *M. abscessus* clinical isolates.** We further assessed the efficacy of the drug combinations against 20 new *M. abscessus* clinical isolates. These isolates were identified to be *M. abscessus* subsp. *abscessus* based on the sequences of the 16S rRNA gene, DNA gyrase subunit B, and DNA-directed RNA polymerase subunit  $\beta$ . The results obtained with these clinical isolates are shown in Fig. 4. The growth inhibition rate by the combination of clofazimine and TB47 was  $68.09\% \pm 17.95\%$ , which was significantly higher than that of either drug alone. The clofazimine-TB47-roxithromycin triple combination further increased the inhibition rate to  $85.24\% \pm 4.97\%$  (Fig. 4).

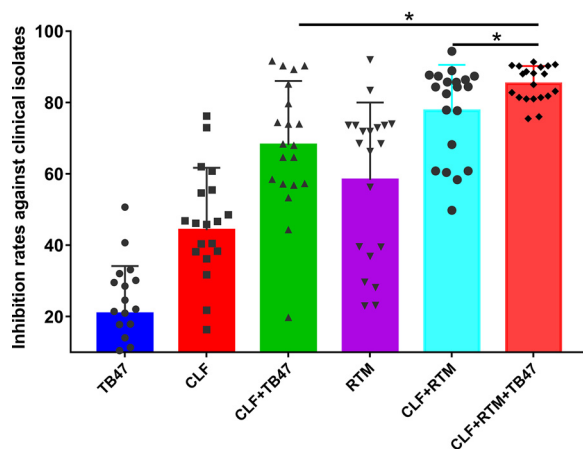


**FIG 4** Efficacy against 20 clinical *M. abscessus* isolates. Clinical isolates of *M. abscessus* were treated with various drugs and combinations, as indicated, for 24 h prior to the measurement of growth inhibition by alamarBlue assay. The inhibition rates were calculated by comparing the fluorescence of a drug-treated group to that of the drug-free control. The concentrations of TB47, clofazimine (CLF), and roxithromycin (RTM) were 1 mg/liter, 1 mg/liter, and 2.5 mg/liter, respectively. \*,  $P < 0.05$  (unpaired  $t$  test).

## DISCUSSION

*M. abscessus* requires 3 to 6 days to form visible colonies on solid medium, rendering the evaluation of drugs time-consuming using the conventional agar proportion method. In this study, we constructed a selectable marker-free, stable autoluminescent *M. abscessus* strain using an integration-proficient plasmid harboring two *dif* sequences, the *apr* gene as the selection marker, and the *int* gene and the *attP* site from mycobacteriophage Tweety. Our initial attempts with plasmids derived from mycobacteriophage L5 or Giles were not successful, suggesting that these integrative plasmids may not be suitable for integration into the genome of the *M. abscessus* GZ002 strain used in the study. Interestingly, when we performed a BLAST search in NCBI using the core *attP* sites of L5 (*attP*<sub>L5</sub>) (5'-TCTTCCAAACTAGCTACGCGGGTTCGATTCCCGTCGCCGCTC-3'), Giles (*attP*<sub>Giles</sub>) (5'-TGACTGGGGTCAAGGGTTCGAGTTCAAATCCTGTAGCCCGAC-3'), and Tweety (*attP*<sub>Tweety</sub>) (5'-GCTGACTCTTAATCAGCGGGTTCGGGGTTCGAAACCTCACGGCGCAC-3') against genome sequences of *M. abscessus*, the *attP*<sub>Tweety</sub> shared 100% identity to some *M. abscessus* strains, but the other two sites affirmed only ~98% identity since 1 base (underlined) was different. The underlined G residues in *attP*<sub>L5</sub> and in *attP*<sub>Giles</sub> were A and T, respectively, in *M. abscessus* genomes. Thus, this could possibly explain why only a Tweety-derived vector worked and why a high degree of identity may be strictly necessary for such an integrative vector to work. The *int*<sub>Tweety</sub> and *apr* in the same cassette were resolved effectively, which meant the *dif* used works efficiently not only in *M. tuberculosis*, *Mycobacterium bovis* BCG, and *Mycobacterium smegmatis* (24) but also in *M. abscessus*. Several luminescent *M. abscessus* strains have been reported. However, they all contained selectable markers (21, 25), making them less suitable for subsequent drug screening/evaluation due to the potential cross-resistance. Here, we report for the first time the construction of a selectable marker-free and stable autoluminescent *M. abscessus* strain, UAImab, based on the *dif*/*Xer* recombinase system (26). Application of the UAImab strain as a reporter allowed us to assess drug activity *in vitro* in  $\leq 9$  h in larger scale. Thus, the development and evaluation of anti-*M. abscessus* drugs, which are of urgent need, can be greatly facilitated.

More importantly, UAImab offers considerable advantages for *in vivo* drug efficacy assessment. In this study, we applied a murine model of acute *M. abscessus* infection. The combination of this model with our autoluminescent strain allowed us to perform a rapid, facile, and noninvasive evaluation of antibiotic activity *in vivo* in the same batch of live mice. On one hand, the simplicity of detecting light production of live mice infected with UAImab obviated the need for CFU measurement, making it possible to

assess *in vivo* drug activity in  $\leq 4$  days with more powerful statistical significance. Furthermore, this noninvasive approach also allowed real-time monitoring of drug activity, as is the case for autoluminescent *M. tuberculosis* and *M. ulcerans* (19, 20), thereby providing a more detailed image of drug activity profiles. Facilitated by this noninvasive approach, we identified that the combination of two mycobacterial ETC-targeting drugs, i.e., clofazimine and TB47, has superior activity against *M. abscessus*, which was further verified in the pulmonary infection model.

It is important to note that in our pulmonary infection model, *M. abscessus* loads in lungs were found to undergo a decline after 1 week of infection even in the immunocompromised nude mice, suggestive of residual immunity capable of controlling the infection. A previous study demonstrated the successful use of nude mice to produce stable chronic *M. abscessus* infection in lungs (27). This inconsistency may be due to the different *M. abscessus* strains used and/or different doses of infection applied.

The ETC of mycobacteria has emerged as the target of many recently developed or repurposed antitubercular drugs. This is exemplified by clofazimine (6), TB47 (14, 15), and Q203 (12). Among these drugs, only clofazimine has been introduced for clinical treatment of *M. abscessus* infection (10) and evaluated for efficacy against *M. abscessus*. A previous report showed that clofazimine was effective against *M. abscessus* under *in vitro* conditions when it was administered alone or in combination with amikacin or clarithromycin (9), making clofazimine a potential drug for treatment of *M. abscessus*. However, the delayed effect of clofazimine reported in *M. tuberculosis* (11) indicates that long-term administration of the drug is necessary, which will, inevitably, lead to more severe adverse effects, such as skin pigmentation (6). It is thus important to know whether clofazimine also has delayed activity against *M. abscessus*. Here, we found that the obvious *in vivo* bactericidal activity of clofazimine occurred only after 2 and 3 weeks of treatment but not within the first week of treatment, suggesting that the drug may have a delayed effect against *M. abscessus*.

Similar to Q203, TB47 targets mycobacterial QcrB, a conservative component of the energy-efficient cytochrome  $bc_1-aa_3$  supercomplex in mycobacteria (12, 14, 15). We reported previously that TB47 is highly bactericidal against *M. ulcerans* (14). In stark contrast, we found that TB47, when administered alone, did not show any effect *in vitro*, suggesting either that TB47 cannot inhibit *M. abscessus* QcrB or that other pathways could alleviate the inhibitory effect of TB47 *in vitro*. Differentiation between these possibilities warrants further investigation. However, we noted that *M. abscessus* QcrB shares only 78% identity with that of *M. tuberculosis*, which is sensitive to TB47 (15). Moreover, QcrB from *Mycobacterium marinum* and *M. ulcerans*, both of which are susceptible to TB47 (14), shares 89% identity with that of *M. tuberculosis*. Mutation of Thr313 in *M. tuberculosis* QcrB (12) and of Thr323 (Thr313 in *M. tuberculosis* QcrB) in QcrB of *M. marinum* and *M. ulcerans* (14) confers resistance to Q203 and TB47, respectively. Importantly, amino acid polymorphism was observed directly after the Thr site, i.e., aspartic acid, in *M. abscessus* QcrB, in contrast to the glutamic acid in the QcrB of *M. tuberculosis*, *M. marinum*, and *M. ulcerans*. Based on these observations, it may be argued that the polymorphism of QcrB could affect the susceptibility of *M. abscessus* to TB47. However, TB47 alone showed *in vivo* activity and synergistic activity with clofazimine, which indicated that TB47 may inhibit the QcrB of *M. abscessus* and affect its growth when the compensatory pathway(s), such as the cytochrome *bd* oxidase (Cyt-*bd*) containing CytAB (14), could not work well.

Dual- and even triple-ETC targeting proved to be an effective approach in *M. tuberculosis*. In particular, combination treatment of clofazimine with cytochrome  $bc_1$  inhibitors (e.g., Q203) was found to exert a markedly enhanced killing of both replicating and nonreplicating *M. tuberculosis* bacteria (16, 17). Furthermore, inhibitors of menaquinone biosynthesis also have enhanced activity when administered in combination with other ETC-targeting drugs, such as clofazimine and QcrB inhibitors (18). These observations led us to investigate in *M. abscessus* the combination activity of clofazimine and TB47, a representative cytochrome  $bc_1$  inhibitor. Interestingly, although TB47 did not inhibit the growth of *M. abscessus* *in vitro*, it showed an inhibitory



**TABLE 2** Primers used in the study

Primer name	Nucleotide sequence (5'–3') <sup>a</sup>
Amf	GATAAGGT <u>ACCC</u> ACCACCGACTATTTG
Amr	CTCCGGGT <u>TACC</u> AGCTCAGCCAATCGAC
16SRNA-F <sup>b</sup>	CAAGTCGAACGGAAAGGC
16SRNA-R <sup>b</sup>	TTACCCGCTGGCAACATA
gyrB-F <sup>b</sup>	ACATCAACCGCACCAAGTCA
gyrB-R <sup>b</sup>	CAGCGTCGGCCATCAACA
rpoB-F <sup>b</sup>	AGCGCATGACCACCCAGGAC
rpoB-R <sup>b</sup>	CATACACCGACAGCGAGCC
attP1Bf	AAGAGCTCTTCTGCGTTTCTTAGTTGCCAT
attP1Br	AAACTCGAGGACATGTAGGACCAAGTAAA
int1Bf	AAATCC <u>CCCGG</u> GATACCAGGAGAAACGTTGTCAA
int1Br	AAAAGCTCTAGACTACGCAAACGTCGATGGGA
AprXF	TTATCTAGACACCACCGACTATTTG
AprXR	TGGTCTAGAAGCTCAGCCAATCGAC
Al1Bf	AAACCCTCACGGCGCACAGGTCA
Al1Br	CGTCAGCAACCAGTTATCCAGCATTTA

<sup>a</sup>Restriction sites are underlined.<sup>b</sup>These primers were used for identifying the clinical *M. abscessus* isolates.

effect on bacterial growth in mice. Furthermore, TB47 also markedly potentiated the activity of clofazimine both *in vitro* and in murine models. In contrast, TB47 did not potentiate the activity of non-ETC-targeting drugs such as clarithromycin, amikacin, and roxithromycin (data not shown). These findings seem to support the idea that *M. abscessus* QcrB can be inhibited by TB47. The lack of growth inhibition phenotype under *in vitro* conditions may be the result of the activation of an unidentified pathway(s) that could exempt the bacteria from TB47-mediated growth inhibition. Another interesting finding is that the combination of clofazimine and TB47 delivered a much earlier effect, suggesting that TB47 also accelerated the activity of clofazimine. This is rather interesting, given the delayed effect of clofazimine. Altogether, our findings seem to emphasize the notion that dual/triple-ETC targeting is an effective therapeutic approach for treating mycobacterial infections. Finally, we found that the addition of roxithromycin, a macrolide drug, to the clofazimine-TB47 combination further enhanced the efficacy. In particular, this triple combination was also effective against 20 clinical isolates of *M. abscessus* subsp. *abscessus*, which is the most frequently found *M. abscessus* subspecies in hospital (28). In addition to the efficacy, addition of a macrolide to the TB47-clofazimine combination may provide a further benefit by limiting the emergence of resistant strains. Indeed, resistance of *M. abscessus* to clofazimine was recently shown to be caused by overexpression of a putative efflux pump, which also mediated coresistance to bedaquiline (29). Whether the same mechanism could affect susceptibility to macrolides remains to be investigated. Based on these results, we propose that regimens based on clofazimine, TB47 (or other cytochrome *bc<sub>1</sub>* inhibitors), and a macrolide should be further exploited to obtain efficient anti-*M. abscessus* regimens.

In conclusion, we have successfully constructed a selectable marker-free autoluminescent *M. abscessus* strain for rapid, convenient, real-time, and noninvasive antibiotic evaluation both *in vitro* and *in vivo*. The noninvasive approach for antibiotic assessment using the autoluminescent strain allowed us to identify that the combination of clofazimine and TB47 is effective against *M. abscessus*. Furthermore, the addition of a macrolide to the combination further enhanced the efficacy.

## MATERIALS AND METHODS

**Bacterial strains, culture conditions, and drug preparations.** *Escherichia coli* DH5 $\alpha$  was grown at 37°C in Luria-Bertani (LB) medium. *M. abscessus* GZ002, a clinical isolate described previously (30), for which the whole genome and DNA methylome have been sequenced and analyzed (31), was used as the parental strain to construct the UAlMab strain. In addition, 20 new clinical strains of *M. abscessus* subsp. *abscessus* isolated from Guangzhou Chest Hospital (Guangzhou, China), as identified by comparison of sequences of the 16S rRNA gene, the DNA gyrase subunit gene, and the DNA-directed RNA polymerase subunit  $\beta$  gene (Table 2 gives primer information), with their corresponding homologous genes in the

reference strain *M. abscessus* ATCC 19977 (30), were investigated in this study. *M. abscessus* strains were grown at 37°C in Middlebrook 7H9 broth (Difco) supplemented with 0.05% Tween 80 and 10% oleic acid-albumin-dextrose-catalase (OADC; Difco), or on Middlebrook 7H11 agar (Difco) supplemented with 10% OADC. Apramycin was used at a concentration of 100 mg/liter for *E. coli* and 240 mg/liter for *M. abscessus*, and hygromycin was used at 200 mg/liter for *E. coli*. Stock solutions of apramycin, gentamicin, kanamycin, and amikacin were prepared in water, and stock solutions of clarithromycin, ceftiofur, and clofazimine were prepared in dimethyl sulfoxide. Hygromycin B was purchased from Roche Diagnostics, and TB47 was obtained from Guangzhou Eggbio, Ltd., China. For *in vivo* studies, clofazimine, TB47, clarithromycin, and roxithromycin were formulated freshly in 0.05% sodium salt of carboxy methyl cellulose (CMC-Na) for oral delivery, and amikacin was formulated in distilled water for subcutaneous injection.

**Construction of the UAIMab strain.** We initially tried to use mycobacteriophage L5-derived vectors (i.e., pMH94 [32] and pOPHI [33]) to transform *M. abscessus* GZ002, but the attempts failed. Subsequently, mycobacteriophage Tweety-derived pTTP1B (34) was used. The procedure for constructing the UAIMab strain is in accordance with our previous work (33). We took advantage of a previously described plasmid, pUCDHmke, which harbors a *dif* sequence (24). The *int* gene from pTTP1B (34) was cloned and inserted into pUCDHmke between *Sma*I and *Xba*I to create pUCDI1B containing *int* flanked by *dif* sequences. The *apr* gene, cloned from pUCDAIm (35), was inserted into pUCDI1B at the *Xba*I site to generate pUCDAI1B. In this plasmid, both *apr* and *int* are located between the two *dif* sequences. The *attP* fragment cloned from pTTP1B was inserted into pOPHI (33), expressing the *luxCDABE* operon under the control of the *hsp60* promoter (36), to create the plasmid pOP1B. The pOP1B plasmid was linearized by *Xho*I digestion, followed by ligation with *Xho*I-digested pUCDAI1B to generate pOPA11B (see Fig. S2 in the supplemental material). The pOPA11B plasmid was sequenced and then electroporated into the parental *M. abscessus* GZ002. The primers used are listed in Table 2.

After electroporation, individual colonies were selected on apramycin-containing 7H11 plates and suspended in 200  $\mu$ l of 7H9 medium, followed by measuring relative light units (RLU) using a luminometer (Promega). The colonies yielding >1,000 RLU/colony, considered to be autoluminescent, were subcultured in drug-free 7H9 medium to allow for the removal of the *dif*-flanked *int*-*apr* sequence (Fig. S2) by endogenous recombinases XerC and XerD (26). The cultures were then diluted and plated onto apramycin-free 7H11 plates, and resultant colonies were streaked on both apramycin-free and apramycin-containing plates. Colonies grown on apramycin-free but not apramycin-containing plates were further examined by PCR using primers AI1Bf and AI1Br (Table 2) to verify the loss of the *int*-*apr* sequence. The PCR products were sequenced.

**Assessment of UAIMab bioluminescence stability.** UAIMab colonies were subcultured in 50 ml of 7H9 medium to an OD<sub>600</sub> of 0.5 to 0.7. Subsequently, 0.5 ml of culture was subgrown in 50 ml of 7H9 medium to mid-exponential phase. This was step repeated for a total of 5 rounds (~30 to 35 generations). Then, cultures were diluted and plated on 7H11 agar. A total of 200 colonies, together with 5 parental *M. abscessus* colonies, were randomly picked and resuspended in 100  $\mu$ l of LB broth for RLU measurement. The percentage of autoluminescent clones was calculated as follows: number of positive clones (defined by yielding an RLU of >1,000 per colony)/total number of colonies examined ( $\times 100\%$ ).

**Growth comparison of UAIMab and the parental *M. abscessus* GZ002.** The growth comparison was performed by culturing the two strains separately and parasynchronously. Log-phase UAIMab and wild-type (WT) *M. abscessus* cultures were diluted to an OD<sub>600</sub> of 0.01, followed by measuring the OD<sub>600</sub> at 3-h intervals. Alternatively, log-phase cultures were diluted by 10<sup>4</sup>-fold, followed by measuring CFU at time points as indicated in Fig. 1B. RLU counts of the UAIMab culture were also recorded.

For assessing *in vivo* growth, mid-log-phase cultures of UAIMab and the parental *M. abscessus* strain were centrifuged and resuspended in phosphate-buffered saline (PBS). Four- to 6-week-old female BALB/c nude mice were infected with 7.5 log<sub>10</sub> CFU via tail vein. Mice were sacrificed for CFU measurement at days 1, 7, and 14 postinfection.

**Drug susceptibility testing.** As defined earlier (14), the MIC determined by RLU measurement was the lowest drug concentration which decreased RLU counts by >90% compared the level of the untreated controls. The assay was performed in 96-well plates. In each well, 196  $\mu$ l of the diluted UAIMab culture (~10<sup>6</sup> CFU/ml) and 4  $\mu$ l of drug were added. RLU values were recorded at 3-h intervals using a plate reader (Envision Multilabel). The MIC determined by the 7H11 agar method was defined as the lowest drug concentration inhibiting at least 99% of bacterial growth observed for drug-free controls (37). The plates were incubated for 4 days before they were read.

Antibiotic efficacy was also tested for 20 clinical *M. abscessus* strains using a microplate alamarBlue assay (38). Log-phase cultures were diluted to an OD<sub>600</sub> of 0.001 (approximately 10<sup>5</sup> CFU/ml). Fixed concentrations of antibiotics were added into 0.2 ml of the diluted culture, followed by the addition, after 24 h of incubation, of 20  $\mu$ l of 10 $\times$  alamarBlue solution (Alamar Biosciences/Accumed, Westlake, Ohio). Twenty-four hours later, fluorescence units (FU) were recorded using a plate reader (Envision Multilabel) with excitation at 530 nm and emission at 590 nm. The inhibition rate was calculated as follows:  $FU_{\text{treated}}/FU_{\text{untreated}} \times 100\%$ .

**RLU and CFU measurement in mice.** Mice were first anesthetized by isoflurane inhalation, and RLU counts were determined, in a noninvasive fashion, by laying the breast of the mouse over the detection hole of a luminometer (Promega) (19). Uninfected mice or mice infected with the WT strain showed a baseline value of approximately 100. In some experiments, mice were euthanized to aseptically harvest lungs and spleens. Organs were homogenized in 2 ml of PBS, followed by serial 10-fold dilutions and plating on 7H11 agar plates. CFU counts were recorded after 6 days of incubation at 37°C. To prevent

possible drug carryover, tissue homogenates of clofazimine-treated mice were plated on 7H11 agar containing 0.4% charcoal, as described previously (11).

**Assessment of drug efficacy in murine model using UAIMab.** Four- to 6-week-old, female, BALB/c nude mice were infected via tail vein with  $7.5 \log_{10}$  CFU of UAIMab. RLU counts of the breast of the live mice were examined 4 h after infection to exclude any mice giving abnormal RLU counts. The mice were administered either 0.05% CMC-Na (negative control) or clofazimine (20 mg/kg/day) and/or TB47 (25 mg/kg/day) freshly prepared in 0.05% CMC-Na once daily via oral gavage. The RLU counts were recorded daily for 4 days.

Alternatively, 4- to 6-week-old, female, BALB/c nude mice were infected by aerosol with  $4.6 \log_{10}$  CFU UAIMab using the Middlebrook inhalation exposure system (Glas-Col). Treatment was initiated after day 1 of infection for 5 consecutive days. Mice were treated with 0.05% CMC-Na, clofazimine (50 mg/kg/day), roxithromycin (120 mg/kg/day), and TB47 (25 mg/kg/day). At time points indicated in Fig. 3D, mice were sacrificed for CFU determination in lungs and spleens. The rate of decrease in the lung bacterial loads was calculated based on viability data (CFU count) of weeks 1, 2, and 3. A linear trend line was made for each group, and the associated slope (i.e., the  $k$  value of the linear line) was obtained and compared with that of the solvent (CMC-Na) control.

**Ethics statement.** Animals were housed and handled in accordance with guidelines set by the Association for the Assessment and Accreditation of Laboratory Animal Care. This study (no. 2016011) was approved by the Ethics Committee of Animal Experiments at Guangzhou Institutes of Biomedicine and Health.

**Statistical analysis.** Data are expressed as means  $\pm$  standard deviations (SD). Student's  $t$  test was used to analyze differences between two groups.  $P$  values of  $<0.05$  were considered to be statistically significant.

**Data availability.** The sequence of pOPA11B was deposited in GenBank under accession number [MG680211](https://www.ncbi.nlm.nih.gov/nuclseq/680211).

## SUPPLEMENTAL MATERIAL

Supplemental material is available online only.

**SUPPLEMENTAL FILE 1**, PDF file, 0.2 MB.

## ACKNOWLEDGMENTS

We thank Graham F. Hatfull (University of Pittsburgh) for generously providing pTTP1B and pGH1000A plasmids. We also thank Xiantao Zhang (Guangzhou Eggbo Co., Ltd.) for offering TB47.

This work was supported by the National Natural Science Foundation of China (81973372, 21920102003), by the National Mega-project of China for Innovative Drugs (grant number 2019ZX09721001-003-003) and for Main Infectious Diseases (2017ZX10302301-003-002), by Chinese Academy of Sciences grants (YJKYYQ20170036 and 154144KYSB20190005), Science and Technology Department of Guangdong Province (2017A020212004, GDME-2018C003, and 2019B110233003), and partially by grants (SKLRD2016ZJ003 and SKLRD-OP-201919) from the State Key Lab of Respiratory Disease, Guangzhou Institute of Respiratory Diseases, First Affiliated Hospital of Guangzhou Medical University. T.Z. received a Science and Technology Innovation Leader of Guangdong Province grant (2016TX03R095). M.M.I. received a CAS-TWAS President Fellowship for International Doctoral Students, and H.M.A.H. received a UCAS Scholarship for International Students.

The funders had no role in study design, data collection and analysis, decision to publish, or preparation of the manuscript.

We declare that we have no conflicts of interest.

An application for a China invention patent for the selectable marker-free autoluminescent *Mycobacterium abscessus* and the techniques for its construction was filed in March 2015 and it was authorized on 7 August 2018 (39). A China invention patent for the new application of pyrazolo[1,5-a]pyridine compounds and a combination of drugs to treat *M. abscessus* infections was filed in 2017 (40).

## REFERENCES

- Lopeman RC, Harrison J, Desai M, Cox J. 2019. *Mycobacterium abscessus*: environmental bacterium turned clinical nightmare. *Microorganisms* 7:90. <https://doi.org/10.3390/microorganisms7030090>.
- Nessar R, Cambau E, Reyat JM, Murray A, Gicquel B. 2012. *Mycobacterium abscessus*: a new antibiotic nightmare. *J Antimicrob Chemother* 67:810–818. <https://doi.org/10.1093/jac/dkr578>.
- Cowman S, van Ingen J, Griffith DE, Loebinger MR, Cowman S, van Ingen J, Griffith DE, Loebinger MR. 2019. Non-tuberculous mycobacterial pulmonary disease. *Eur Respir J* 54:1900250. <https://doi.org/10.1183/13993003.00250-2019>.
- Wu ML, Aziz DB, Dartois V, Dick T. 2018. NTM drug discovery: status, gaps and the way forward. *Drug Discov Today* 23:1502–1519. <https://doi.org/10.1016/j.drudis.2018.04.001>.

5. WHO. 2019. Global tuberculosis report 2019. [https://www.who.int/tb/publications/global\\_report/en/](https://www.who.int/tb/publications/global_report/en/).
6. Yano T, Kassovska-Bratinova S, Teh JS, Winkler J, Sullivan K, Isaacs A, Schechter NM, Rubin H. 2011. Reduction of clofazimine by mycobacterial type 2 NADH:quinone oxidoreductase: a pathway for the generation of bactericidal levels of reactive oxygen species. *J Biol Chem* 286: 10276–10287. <https://doi.org/10.1074/jbc.M110.200501>.
7. Pang Y, Zong Z, Huo F, Jing W, Ma Y, Dong L, Li Y, Zhao L, Fu Y, Huang H. 2017. *In vitro* drug susceptibility of bedaquiline, delamanid, linezolid, clofazimine, moxifloxacin, and gatifloxacin against extensively drug-resistant tuberculosis in Beijing, China. *Antimicrob Agents Chemother* 61:e00900-17. <https://doi.org/10.1128/AAC.00900-17>.
8. Grosset JH, Tyagi S, Almeida DV, Converse PJ, Li SY, Ammerman NC, Bishai WR, Enarson D, Trebuchq A. 2013. Assessment of clofazimine activity in a second-line regimen for tuberculosis in mice. *Am J Respir Crit Care Med* 188:608–612. <https://doi.org/10.1164/rccm.201304-0753OC>.
9. Ferro BE, Meletiadiis J, Wattenberg M, de Jong A, van Soolingen D, Mouton JW, van Ingen J. 2016. Clofazimine prevents the regrowth of *Mycobacterium abscessus* and *Mycobacterium avium* type strains exposed to amikacin and clarithromycin. *Antimicrob Agents Chemother* 60:1097–1105. <https://doi.org/10.1128/AAC.02615-15>.
10. Yang B, Jhun BW, Moon SM, Lee H, Park HY, Jeon K, Kim DH, Kim SY, Shin SJ, Daley CL, Koh WJ. 2017. Clofazimine-containing regimen for the treatment of *Mycobacterium abscessus* lung disease. *Antimicrob Agents Chemother* 61:e02052-16. <https://doi.org/10.1128/AAC.02052-16>.
11. Ammerman NC, Swanson RV, Tapley A, Moodley C, Ngcobo B, Adamson J, Dorasamy A, Moodley S, Mgaga Z, Bester LA, Singh SD, Almeida DV, Grosset JH. 2017. Clofazimine has delayed antimicrobial activity against *Mycobacterium tuberculosis* both *in vitro* and *in vivo*. *J Antimicrob Chemother* 72:455–461. <https://doi.org/10.1093/jac/dkw417>.
12. Pethe K, Bifani P, Jang J, Kang S, Park S, Ahn S, Jiricek J, Jung J, Jeon HK, Cechetto J, Christophe T, Lee H, Kempf M, Jackson M, Lenaerts AJ, Pham H, Jones V, Seo MJ, Kim YM, Seo M, Seo JJ, Park D, Ko Y, Choi I, Kim R, Kim SY, Lim S, Yim S-A, Nam J, Kang H, Kwon H, Oh C-T, Cho Y, Jang Y, Kim J, Chua A, Tan BH, Nanjundappa MB, Rao SPS, Barnes WS, Wintjens R, Walker JR, Alonso S, Lee S, Kim J, Oh S, Oh T, Nehrbass U, Han S-J, No Z, Lee J, Brodin P, Cho S-N, Nam K, Kim J. 2013. Discovery of Q203, a potent clinical candidate for the treatment of tuberculosis. *Nat Med* 19:1157–1160. <https://doi.org/10.1038/nm.3262>.
13. Tang J, Wang B, Wu T, Wan J, Tu Z, Njire M, Wan B, Franzblauc SG, Zhang T, Lu X, Ding K. 2015. Design, synthesis, and biological evaluation of pyrazolo[1,5-a]pyridine-3-carboxamides as novel antitubercular agents. *ACS Med Chem Lett* 6:814–818. <https://doi.org/10.1021/acsmedchemlett.5b00176>.
14. Liu Y, Gao Y, Liu J, Tan Y, Liu Z, Chhotaray C, Jiang H, Lu Z, Chiwala G, Wang S, Makafe G, Islam MM, Hameed HMA, Cai X, Wang C, Li X, Tan S, Zhang T. 2019. The compound TB47 is highly bactericidal against *Mycobacterium ulcerans* in a Buruli ulcer mouse model. *Nat Commun* 10:524. <https://doi.org/10.1038/s41467-019-08464-y>.
15. Lu X, Williams Z, Hards K, Tang J, Cheung CY, Aung HL, Wang B, Liu Z, Hu X, Lenaerts A, Woolhisler L, Hastings C, Zhang X, Wang Z, Rhee K, Ding K, Zhang T, Cook GM. 2019. Pyrazolo[1,5-a]pyridine inhibitor of the respiratory cytochrome bcc complex for the treatment of drug-resistant tuberculosis. *ACS Infect Dis* 5:239–249. <https://doi.org/10.1021/acscinfed.8b00225>.
16. Berube BJ, Parish T, Berube BJ, Parish T. 2018. Combinations of respiratory chain inhibitors have enhanced bactericidal activity against *Mycobacterium tuberculosis*. *Antimicrob Agents Chemother* 62:e01677-17. <https://doi.org/10.1128/AAC.01677-17>.
17. Lamprecht DA, Finin PM, Rahman MA, Cumming BM, Russell SL, Jonnal SR, Adamson JH, Steyn AJ. 2016. Turning the respiratory flexibility of *Mycobacterium tuberculosis* against itself. *Nat Commun* 7:12393. <https://doi.org/10.1038/ncomms12393>.
18. Berube BJ, Russell D, Castro L, Choi S-R, Narayanasamy P, Parish T. 2019. Novel MenA inhibitors are bactericidal against *Mycobacterium tuberculosis* and synergize with electron transport chain inhibitors. *Antimicrob Agents Chemother* 63:e02661-18. <https://doi.org/10.1128/AAC.02661-18>.
19. Zhang T, Li SY, Nuermberger EL. 2012. Autoluminescent *Mycobacterium tuberculosis* for rapid, real-time, non-invasive assessment of drug and vaccine efficacy. *PLoS One* 7:e29774. <https://doi.org/10.1371/journal.pone.0029774>.
20. Zhang T, Li SY, Converse PJ, Grosset JH, Nuermberger EL. 2013. Rapid, serial, non-invasive assessment of drug efficacy in mice with autoluminescent *Mycobacterium ulcerans* infection. *PLoS Negl Trop Dis* 7:e2598. <https://doi.org/10.1371/journal.pntd.0002598>.
21. Gupta R, Netherton M, Byrd TF, Rohde KH. 2017. Reporter-based assays for high-throughput drug screening against *Mycobacterium abscessus*. *Front Microbiol* 8:2204. <https://doi.org/10.3389/fmicb.2017.02204>.
22. Lu X, Tang J, Cui S, Wan B, Franzblauc SG, Zhang T, Zhang X, Ding K. 2017. Pyrazolo[1,5-a]pyridine-3-carboxamide hybrids: design, synthesis and evaluation of anti-tubercular activity. *Eur J Med Chem* 125:41–48. <https://doi.org/10.1016/j.ejmech.2016.09.030>.
23. Berube BJ, Castro L, Russell D, Ovechkina Y, Parish T. 2018. Novel screen to assess bactericidal activity of compounds against non-replicating *Mycobacterium abscessus*. *Front Microbiol* 9:2417. <https://doi.org/10.3389/fmicb.2018.02417>.
24. Mugweru J, Makafe G, Cao Y, Zhang Y, Wang B, Huang S, Njire M, Chhotaray C, Tan Y, Li X, Liu J, Tan S, Deng J, Zhang T. 2017. A cassette containing thiostrepton, gentamicin resistance genes, and dif sequences is effective in construction of recombinant *Mycobacteria*. *Front Microbiol* 8:468. <https://doi.org/10.3389/fmicb.2017.00468>.
25. Meir M, Grosfeld T, Barkan D, Meir M, Grosfeld T, Barkan D. 2018. Establishment and validation of *Galleria mellonella* as a novel model organism to study *Mycobacterium abscessus* infection, pathogenesis, and treatment. *Antimicrob Agents Chemother* 62:e02539-17. <https://doi.org/10.1128/AAC.02539-17>.
26. Cascioferro A, Boldrin F, Serafini A, Provedi R, Palu G, Manganelli R. 2010. Xer site-specific recombination, an efficient tool to introduce unmarked deletions into mycobacteria. *Appl Environ Microbiol* 76: 5312–5316. <https://doi.org/10.1128/AEM.00382-10>.
27. Lerat I, Cambau E, Roth Dit Bettoni R, Gaillard JL, Jarlier V, Truffot C, Veziris N. 2014. *In vivo* evaluation of antibiotic activity against *Mycobacterium abscessus*. *J Infect Dis* 209:905–512. <https://doi.org/10.1093/infdis/jit614>.
28. Davidson RM. 2018. A closer look at the genomic variation of geographically diverse *Mycobacterium abscessus* clones that cause human infection and disease. *Front Microbiol* 9:2988. <https://doi.org/10.3389/fmicb.2018.02988>.
29. Richard M, Gutierrez AV, Viljoen A, Rodriguez-Rincon D, Roquet-Baneres F, Blaise M, Everal I, Parkhill J, Floto RA, Kremer L. 2019. Mutations in the MAB\_2299c TetR regulator confer cross-resistance to clofazimine and bedaquiline in *Mycobacterium abscessus*. *Antimicrob Agents Chemother* 63:e01316-18. <https://doi.org/10.1128/AAC.01316-18>.
30. Guo J, Wang C, Han Y, Liu Z, Wu T, Liu Y, Liu Y, Tan Y, Cai X, Cao Y, Wang B, Zhang B, Liu C, Tan S, Zhang T. 2016. Identification of lysine acetylation in *Mycobacterium abscessus* sing LC-MS/MS after immunoprecipitation. *J Proteome Res* 15:2567–2578. <https://doi.org/10.1021/acs.jproteome.6b00116>.
31. Chhotaray C, Wang S, Tan Y, Ali A, Shehroz M, Fang C, Liu Y, Lu Z, Cai X, Hameed HMA, Islam MM, Surineni G, Tan S, Liu J, Zhang T. 2019. Comparative analysis of whole-genome and methylome profiles of a smooth and a rough *Mycobacterium abscessus* clinical strain. *G3 (Bethesda)* 2019:g3.400737.2019. <https://doi.org/10.1534/g3.119.400737>.
32. Lee MH, Pascopella L, Jacobs WR, Jr, Hatfull GF. 1991. Site-specific integration of mycobacteriophage L5: integration-proficient vectors for *Mycobacterium smegmatis*, *Mycobacterium tuberculosis*, and bacille Calmette-Guerin. *Proc Natl Acad Sci U S A* 88:3111–3115. <https://doi.org/10.1073/pnas.88.8.3111>.
33. Yang F, Njire MM, Liu J, Wu T, Wang B, Liu T, Cao Y, Liu Z, Wan J, Tu Z, Tan Y, Tan S, Zhang T. 2015. Engineering more stable, selectable marker-free autoluminescent mycobacteria by one step. *PLoS One* 10:e0119341. <https://doi.org/10.1371/journal.pone.0119341>.
34. Pham TT, Jacobs-Sera D, Pedulla ML, Hendrix RW, Hatfull GF. 2007. Comparative genomic analysis of mycobacteriophage Tweety: evolutionary insights and construction of compatible site-specific integration vectors for mycobacteria. *Microbiology* 153:2711–2723. <https://doi.org/10.1099/mic.0.2007/008904-0>.
35. Liu T, Wang B, Guo J, Zhou Y, Julius M, Njire M, Cao Y, Wu T, Liu Z, Wang C, Xu Y, Zhang T. 2015. Role of *folP1* and *folP2* genes in the action of sulfamethoxazole and trimethoprim against *Mycobacteria*. *J Microbiol Biotechnol* 25:1559–1567. <https://doi.org/10.4014/jmb.1503.03053>.
36. Stover CK, de la Cruz VF, Fuerst TR, Burlein JE, Benson LA, Bennett LT, Bansal GP, Young JF, Lee MH, Hatfull GF, Snapper SB, Barletta RG, Jacobs WR, Jr, Bloom BR. 1991. New use of BCG for recombinant vaccines. *Nature* 351:456–460. <https://doi.org/10.1038/351456a0>.
37. Zhang T, Bishai WR, Grosset JH, Nuermberger EL. 2010. Rapid assessment of antibacterial activity against *Mycobacterium ulcerans* by using recom-

- binant luminescent strains. *Antimicrob Agents Chemother* 54: 2806–2813. <https://doi.org/10.1128/AAC.00400-10>.
38. Collins L, Franzblau SG. 1997. Microplate alamar blue assay versus BACTEC 460 system for high-throughput screening of compounds against *Mycobacterium tuberculosis* and *Mycobacterium avium*. *Antimicrob Agents Chemother* 41:1004–1009. <https://doi.org/10.1128/AAC.41.5.1004>.
39. Zhang T, Cao Y, Wu T, Tan S, Tan Y, Cai X, Liu C. 7 August 2018. Construction of marker-free self-luminous *Mycobacterium abscessus* and establishment of a high throughput screen model *in vitro*. Chinese patent ZL 201510104936.3.
40. Zhang T, Liu Y, Tan S, Liu J, Li X, Wang B, Zhou P, Cai X, Guo L, Liu Y, Liu Z, Tang Y, Gao Y, Jiang H. 13 April 2017, filing date. New applications of pyrazolo[1,5-a]pyridine compounds and a pharmaceutical composition for treatment of *Mycobacterium abscessus* infection. Chinese patent 201710240224.3.